Characterization of Diffusion-Controlled Mass Transport through Nanoporous and Nanothin Films Plasma Polymerized on a Sputtered Platinum Electrode

Hitoshi Muguruma,* Nobuaki Itazu, and Satoshi Miura

Department of Electronic Engineering, Shibaura Institute of Technology, 3-9-14 Shibaura, Minato-ku, Tokyo 108-8548, Japan

Received: March 14, 2005; In Final Form: August 5, 2005

We demonstrate the diffusion mode of various redox chemical species through a plasma-polymerized nanothin coating with nanometer-sized pores on a sputtered platinum (Pt) electrode. In this work, hexamethyldisiloxane plasma-polymerized films (PPFs) were added onto the sputtered platinum film, both of which were sequentially deposited in the same vacuum chamber. Results of atomic force microscopy, X-ray photoelectron spectroscopy, and electrochemical studies showed that the PPF provided the platinum electrode with a coating with a complete surface coverage. Sub-nanometer-sized pores (less than 1 nm) responsible for a highly crosslinked polymer network in the PPF coatings offered diffusivity-controlled permeation of redox molecules (i.e., size-exclusivity) rather than solubility-controlled permeation (i.e., chemoselectivity). Consequently, variation of the plasma power could give control over the size of the nanometer-sized cavities.

1. Introduction

To date, a plasma-polymerized film (PPF) is studied by many researchers as a new type of polymer thin film.[1−4] It is prepared in a vapor phase under glow discharge or plasma. The resulting film is directly formed onto a substrate as a nanothin coating. The main structural difference between PPFs and conventional polymer films is that the former tends to form an irregular crosslinked network in a three-dimensional build, whereas the latter has a periodicity with a repeating unit.

Typical applications for PPF were gas separation[5−7] and reverse osmosis membrane.[8−10] In these cases, the PPFs were deposited onto porous substrate (25 nm of pore size) such as silica, cellulose, and polysulfone.[5−10] Therefore, control of the expression of functionality is attributed to the pore covered when individual grains coalesce over. To the other hand, PPF, regarded as flat and pinhole free, is deposited onto a nonporous inert surface such as silicon substrate and a sputtering metal surface.[11] Such application of the PPF includes a coating against metal corrosion.[12,13] Also, the unique structures of the nanothin coatings on noble metal electrodes allow for electrochemical applications such as chemical sensors[14,15] and biosensors.[16,17] We focus on the pristine PPF having a nanoporous structure.

We previously reported the size-exclusive mass transport of electrochemical species through acetonitrile and hexadiene PPF coatings on a platinum-sputtered electrode, due to the nanoporous nature of their structures.[18] In this work, we show that the size of the nanopores is controllable upon plasma polymerization, using hexamethlydisiolxane (HMDS) as a model monomer. For the sake of characterization, we performed surface analyses of several PPFs prepared on thin film platinum electrodes using AFM and XPS. Second, electrochemical studies of the PPFs were carried out, using chemical species with a variety of sizes such as hydrogen peroxide (FW 34.01), catechol (FW 110.1), L-ascrobic acid (FW 176.1), and chlorpromazine hydrochloride (FW 355.3).

* To whom correspondence should be addressed. E-mail: muguruma@sic.shibaura-it.ac.jp.

2. Experimental Section

2.1. Materials. Distilled water, sodium dihydrogenphosphate, disodium hydrogenphospate, and hydrogen peroxide were purchased from Kanto chemical (Tokyo, Japan). L-Ascorbic acid, catechol, and chlorpromazine (2-chloro-10-[3-dimethylaminopropyl]phenothiazine) hydrochloride were purchased from Sigma (St. Louis, MO). Hexamethyldisiloxane (HMDS) was purchased from Aldrich (Milwaukee, WI). All reagents used in this work were prepared without further purification.

2.2. Fabrication. Glass slides used to make thin film electrodes were cleaned in 50% nitric acid for 1 h and then rinsed with water and acetone. Platinum thin films were sputtered with an apparatus manufactured by Ulvac, Inc. (VEP-1000, Tokyo, Japan). To improve the adhesion of the platinum films onto the glass substrates, a 30 nm thin chromium film was deposited between the platinum and the glass. The thickness of the platinum (Pt) film (300 nm) was later determined by using a surface profiler (Dektak ST, Veeco Instruments Inc., Tokyo, Japan) and quartz crystal microbalance. Immediately after the platinum deposition, a PPF was additionally deposited with the reactor chamber left evacuated.

The plasma apparatus employed in this study was also from Ulvac, Inc. (VEP-1000, Tokyo, Japan). Substrates were placed in the center of the plasma reactor and 50 mm above the edge of the plasma gun. The monomer was placed in a bottle reservoir. The reactor chamber was evacuated at a base pressure below 10^{-3} Pa. Subsequently, the monomer was supplied to the chamber, whose pressure was controlled under desired conditions. In this experiment, the pressure was fixed at 0.6 Pa and the plasma powers were set at various powers: 100 W (rate: 4.3 ± 0.4 nm/min), 150 W (rate: 16.8 ± 1.7 nm/min), 200 W (rate: 22.2 ± 2.3 nm/min), or 250 W (rate: 27.6 ± 2.8 nm/min). After the monomer flow was stopped as programmed, the reactor was kept to retain the base pressure. For removing the substrates from the reactor, the reactor was filled with air up to the atmospheric pressure. They were usually stored in a desiccator until use. For an experiment, they were immersed in

10.1021/jp051312x CCC: $30.25
Published on Web 09/15/2005

a buffer for an hour to wash off the residual trace of the monomer on the film.

2.3. Measurements. The thickness of the PPFs coated on Pt electrodes was determined by ellipsometry (Ulvac Inc., Tokyo, Japan). Electrochemical studies were performed with a potentiostat (model ALS-701A) from Bioanalytical Systems, Inc. (West Lafayette, IN). The three-electrode configuration was arranged with a Ag/AgCl reference electrode (RE-1C, BAS), a platinum wire counter electrode, and a Pt working electrode with the HMDS PPF (area was 0.25 cm^2). Measurements were made in a 5-mL container at laboratory ambient temperature (25 °C). The supporting electrolyte was a phosphate buffer (20 mM, pH 7.0). Cyclic voltammetry was performed between 0 and 1000 mV (vs Ag/AgCl, 50 mV s^{-1}). Every other cycle was recorded until observed currents became stabilized.

The diffusion of analyte molecules through a PPF can be represented as a simple first-order diffusion equation based upon Fick's First Law of Diffusion. The flux can be generated by application of a potential step and thus be measured by chronocoulometry. The relevant expression is as follows[19]

$$Ji = Di\frac{Ci_2 - Ci_1}{d} \tag{1}$$

where Ji is a flux of an analyte i, Ci_1 is its local concentration close to the electrode determined electrochemically, Ci_2 is its bulk concentration, Di is its diffusion constant, and d is the thickness of the PPF. It is intuitively understandable that the sensitivity of any analyte would decrease with the increase of the thickness of a film coated on an electrode. Actually, the sensitivity toward the analyte i may be defined from this equation, assuming the local concentration of the analyte on the electrode to be zero ($Ci_1 = 0$). In other words, the sensitivity (Ji/Ci_2) toward the analyte i is defined as the mass transport influx of the analyte per the unit bulk concentration, which represents the magnitude of the unit chemical potential created between the bulk phase and the interfacial membrane surface due to electrochemical depletion of the analyte i.

$$\frac{Ji}{Ci_2} = \frac{Di}{d} \tag{2}$$

From eq 2, it is obvious that the sensitivity is proportional to the inverse of the coating thickness. In most cases, the apparent diffusion constant of an electrochemically active chemical species is considered to depend on the coating thickness. Therefore, this equation may be defined as

$$Pi \equiv \frac{Di}{d} \tag{3}$$

where Pi is the diffusive permeability of an analyte i. Combination of (2) and (3) leads to

$$\frac{Ji}{Ci_2} = Pi(d) \tag{4}$$

meaning Pi is a function of d. To rule out the reaction of the PPF-modified electrode and its partition effect between the bulk and the membrane, its sensitivity was estimated by adjustment using the counterpart bare electrode as a reference.

Chronocoulometric measurements were also carried out to evaluate the diffusion coefficient of each analyte passing through the film. A potential step between 0 and +700 mV (vs Ag/AgCl) was applied to the working electrode with the sampling interval of 10 ms. The diffusion coefficient of an analyte i was determined with integrated the Cottrell equation:[20]

$$Qi_t = \frac{2nFACiD^{1/2}t^{1/2}}{\pi^{1/2}} + nFA\Gamma_0 + Q_{dl} \tag{5}$$

where n is the number of electrons transferred to the electrode, F is the Faraday constant, A is the area of the electrode, Ci is the concentration of an analyte i in the film, t is the time after the potential step, Γ_0 is the surface concentration of the analyte, and Q_{dl} is the double-layer charge. Measured currents were observed linearly proportional to the concentration of any analyte, which implies diffusion-limited conditions.

Atomic force microscopy (AFM) was employed to understand the topography of the PPF coatings. Measurements were made in the tapping mode in normal atmosphere using a commercial system (NanoScope IIIaAFM Dimension 3000 stage system, Nihon Veeco KK, Tokyo, Japan). A scanning tip was equipped with an AC mode super sharp chip, which was purchased from Nanosensors Inc. (Neuchatel, Switzerland). The scanning rate was 0.6 Hz. The software dedicated to the AFM system was used to analyze imaging data to calculate the defined informative features such as the root-mean-square roughness values (R_q), the arithmetic mean of the departure of the roughness profile from the mean line (R_a), and the maximum Z-range values (R_{max}). 2D isotropical power spectral densities $P(s)$ were computed as follows:

$$P(s) = \frac{1}{A_i}\left|\int_{A_i} h_i(x,y)\exp(2\pi j(S_x x + S_y y))\,dx\,dy\right|^2 \tag{6}$$

where $h_i(x,y)$ are the height data and A_i is the surface of the image.

The XPS equipment (model: ESCA LAB200iXL) was obtained from Thermo Electron Corp (Waltham, MA) and an Al Kα (1486.6 eV) X-ray source was used. The photoelectron takeoff angle was 90°. The X-ray beam diameter was 1 mm. The X-ray source was operated at 30 W and the pressure during the measurement was less than 1×10^{-4} Pa. To determine a stoichiometric ratio, we compared the signal intensities of the relevant atoms among one another. The relative sensitivity factors were as follows: C 1s, 1.00; O 1s, 2.64; Si 2p, 1.00; and Pt $4f_{7/2}$, 10.2.[21] The full-scan and core-level spectra were recorded in steps of 1 and 0.1 eV, respectively.

3. Results and Discussion

3.1. Characterization of Plasma-Polymerized Coatings on a Sputtered Pt Electrode. The plasma-polymerized parameters that affected the resulting film structure are the plasma power, the monomer flow rate, and the chamber pressure. In this experiment, we tried to optimize only the power (100, 150, 200, and 250 W, respectively) as a parameter with a fixed pressure (0.6 Pa). There was no need to consider the flow rate because the HMDS monomer has an adequate vapor pressure and its bottle was directly connected to the reaction chamber. The PPF were deposited as a thin coating on each substrate, which at the beginning was exposed to a glow discharge of the organic monomer gas. The resulting coatings had, in most cases, a highly branched and cross-linked network structure, making the mass transport along the membrane dominated by the size-exclusivity rather than the chemoselectivity.

In the plasma polymerization, the obtained structure is not necessarily based upon that of the original monomer, because the process occurs via random generation of unstable intermedi-

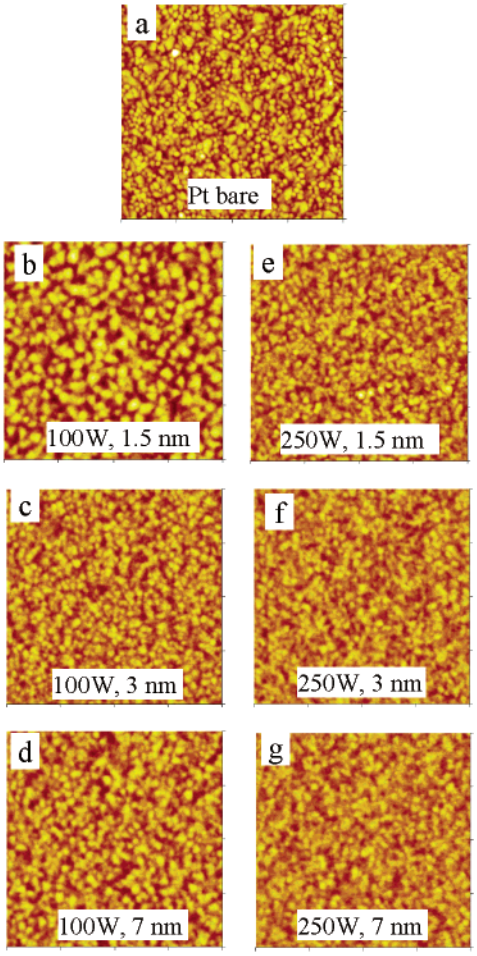

Figure 1. Tapping mode AFM image of HMDF PPF-coated on sputtered Pt: (a) bare Pt. Power and coating thickness were (b) 100 W and 1.5 nm, (c) 100 W and 3 nm, (d) 100 W and 7 nm, (e) 250 W and 1.5 nm, (f) 250 W and 3 nm, and (g) 250 W and 7 nm, respectively. Pressure: 0.6 Pa. Image size: 1 μm. *z*-scale (contrast): 10 nm. Scan rate: 0.6 Hz. Surface data: R_q = (a) 1.01, (b) 1.13, (c) 0.83, (d) 0.75, (e) 0.79, (f) 0.66, and (g) 0.64 nm; R_a = (a) 0.80, (b) 0.92, (c) 0.66, (d) 0.60, (e) 0.62, (f) 0.53, and (g) 0.52 nm.

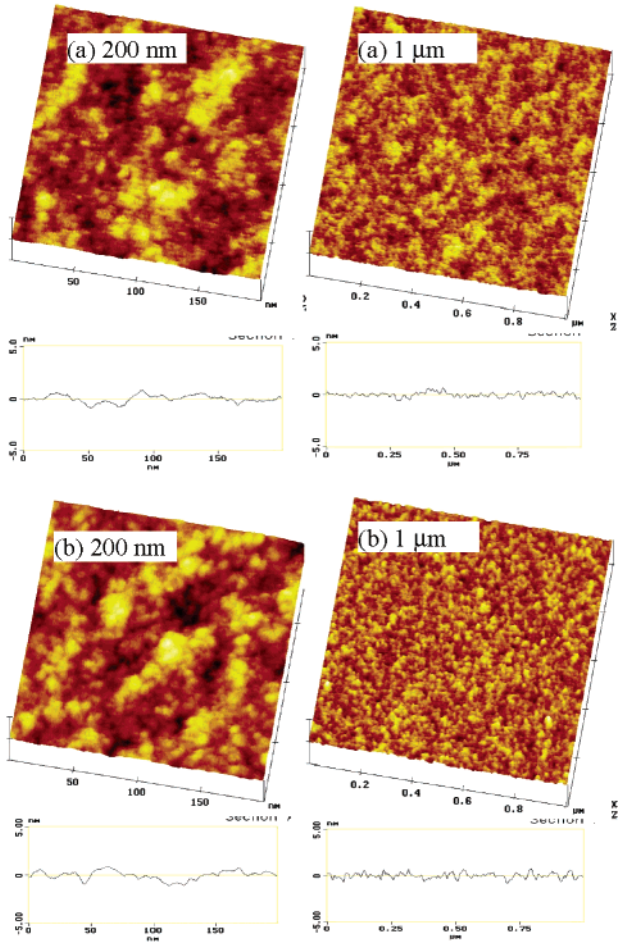

Figure 2. Tapping mode AFM topographical image and cross-sectional profile of HMDS PPF coated on silicon substrate. Image size: 200 nm and 1 μm. *z*-scale (contrast): 10 nm. Scan rate: 0.6 Hz. Film thickness: 7 nm. Polymerization power was (a) 100 and (b) 250 W. Surface data: R_q = (a) 0.28 nm (200 × 200 nm^2), 0.26 nm (1 × 1 μm^2), (b) 0.35 nm (200 × 200 nm^2), 0.30 nm (1 × 1 μm^2); R_a = (a) 0.23 nm (200 × 200 nm^2), 0.21 nm (1 × 1 μm^2), (b) 0.27 nm (200 × 200 nm^2), 0.24 nm (1 × 1 μm^2).

ate species under high-energy plasma.[22] The HMDS PPF has a variety of network conformations with a number of silicon atoms surrounded by oxygen atoms and methyl groups (e.g., $Si(-CH_3)_3(-O-)$, $Si(-CH_3)_2(-O-)_2$, $Si(-CH_3)(-O-)_3$, $Si(-O-)_4$),[23] creating highly hydrophobic surfaces.[22] Krishnamurthy reported[23] that enhancement of the plasma power resulted in increases in the chain length and the number of cross-linked networks of polysiloxane as indicated by widening and splitting of Si−O stretching absorption in IR spectra. This means that the plasma power could affect the average pore size on a nanometer scale.

Figure 1 shows AFM surface images (1 × 1 μm^2) of HMDS PPF coatings, in which no distinct pinholes and defects were observed. A difference in the plasma power (250 and 100 W) gave the corresponding difference in the coating thickness. Also, the thicker the plasma coating was deposited, the smoother became the surface roughness. The surface roughness in the 7-nm-thick coatings was $R_q = 0.6-0.8$ nm. In the 1.5-nm-thick coatings, the surface coated at 250 W was observed to be smoother than that coated at 100 W. This means that in the case of the 1.5-nm-thick coating, the 100-W power was incapable of producing granules large enough to make a smooth surface. In detail, if the roughness of the Pt electrode surface is comparable to the granule size and the thickness of a deposited layer (in the vertical direction), the resulting plasma polymer cannot compensate for such roughness.

Figure 2 shows the AFM surface image with two different scales (200 × 200 nm^2 and 1 × 1 μm^2) and their cross-sectional profile of "pristine" HMDS PPF deposited onto silicon substrate by 100 and 250 W of power. The pinholes and defects are observed in neither of the imaging scales, probably because the surface roughness of less than 1 nm is similar to those of silicon[11] and mica.[24,25] There is no distinct difference between the plasma powers of 100 and 250 W with the values of R_q and R_a, providing the vertical information. On the other hand, the power spectral density (PSD) analysis quantitatively evaluates the average grain size, i.e., the horizontal information. Figure 3 shows a log−log plot with the 2-dimensional isotropic PSD curves calculated from the AFM image (200 nm scale). The PSD intensity of the PPF deposited by 250 W is larger than that deposited by 100 W in the wavelength range between 8 and 60 nm, suggesting that the grain size of the 250-W PPF is slightly larger than that of the 100-W PPF. This tendency was similarly observed in cases of PPFs made from different kinds of monomers.[4,26,27] During the course of plasma polymerization, as a matter of fact, the balance among agglomerization, polymerization, and ablation is important as a resultant effect of various plasma generation conditions. As such, this is strongly

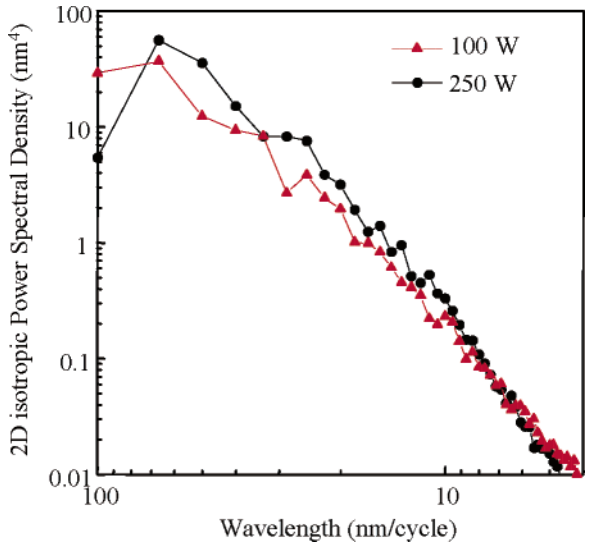

Figure 3. Log−log plot of 2D isotropic PSD curves calculated from AFM measurement based on the data of Figure 2 (200 × 200 nm²).

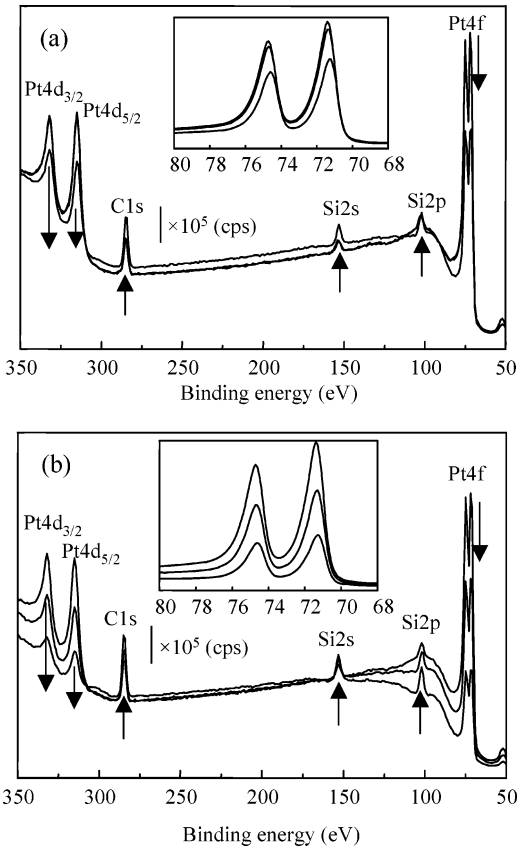

Figure 4. XPS full spectra of HMDS PPF coating on Pt electrode. The direction of the arrows represents the increment of coating thickness (1.5, 3, and 7 nm). Polymerization power was (a) 100 and (b) 250 W. Inset: Core level spectra of Pt 4f.

related to the pore size of the resultant polymer film. However, it is too small to be detected with this experimental technique.

Figure 4 shows XPS data of HMDS PPF coatings with various thicknesses, deposited at 100 and 250 W. Their stoichiometric ratios are summarized in Table 1. The peak due to Pt atoms decreases and the peaks due to carbon 1s and Si atoms increase with the coating thickness. The attenuation of the Pt signal is caused by the HMDS PPF overlayer and related to the film thickness. As a quantitative expression, the following equation represents that the intensity of a photoelectron colliding into a polymer membrane is exponentially decayed compared with that of a bare electrode:

TABLE 1: Elemental Percentage Determined from XPS

surface power, thickness	atom (%)			
	Pt	C	Si	O
100 W, 1.5 nm	28.3	34.9	12.0	24.8
100 W, 3 nm	28.7	39.0	10.6	21.7
100 W, 7 nm	16.1	44.4	17.2	22.3
250 W, 1.5 nm	24.8	41.4	12.6	21.1
250 W, 3 nm	15.7	48.3	14.6	21.4
250 W, 7 nm	7.0	51.9	20.3	20.9

$$I_{\mathrm{Pt,coating}} = I_{\mathrm{Pt,bare}} \exp[-d/(\lambda \sin\theta)] \quad (7)$$

where d is the coating thickness, λ is the mean free path of a Pt photoelectron, and θ is the photoelectron takeoff angle (90° in this experiment). On the other hand, λ (in nm) of an organic compound may be expressed as[28]

$$\lambda = 49/\rho E^2 + 0.11E^{0.5}/\rho \quad (8)$$

where ρ is the bulk density of the organic compound (g/cm³) and E is the electron kinetic energy (eV). By replacing E in eq 7 with an experimental value and assuming $\rho = 0.98$ g/cm³ in the case of poly(dimethylsiloxane), the λ of Pt is estimated to be 3.5 nm. Therefore, the Pt 4f signal ratio between the 3- and 7-nm coatings roughly obeyed the attenuation model represented by eq 7.

The surface characterization data shown in Figures 1−4 provide the evidence that a complete, uniform, and nanothin coating was deposited on a platinum electrode. This is also supported by our observation that electrochemical measurements revealed a far more dramatic change in the case of the PPF-coated electrodes than that of the bare ones.

3.2. Control of Size-Selective Permeation through PPF Coatings. The HMDS PPF did not swell in an aquous solvent probably because of its chemical structure, whereas conventional polymers that have a linear chain structure are prone to swelling; the oxidation current baseline remained stable upon application of a constant potential (+600 mV) and no catastrophic damage was observed at least for 30 repetitions of a cyclic voltammetric (CV) scan. This indicates that the pristine PPF strongly adhered onto the substrate and was robust enough under our experimental conditions.

Actually, cyclic voltammetry was used to measure the oxidation current of various analytes. Figure 5 shows the cyclic voltammograms of hydrogen peroxide obtained with the bare and the PPF-coated electrodes. This analyte is completely oxidized at a polarized potential greater than +500 mV, partially contributed from the catalytic effect of the platinum.[29] With the plasma polymerization coating, the electrode showed a base current lower than that of the bare electrode. Upon addition of hydrogen peroxide, however, a cyclic voltammogram using the PPF-coated electrode showed a drastic increase in the height of its characteristic peak, which was distinctively different from that of the bare electrode. This suggests that the PPF coating may work as a size-exclusive filter for nanometer-sized chemical species at a passive mass transport, which is made possible by the crucial nature of the PPF as a defect-free coating. Since the catalytic capability of a Pt electrode depends on surface properties such as the roughness and the oxidation state,[29] the PPF coating can protect the electrode surface from unwanted and uncontrollable oxidation, enabling creation of electrodes with reproducible surfaces. Here one might imagine even advanced protocols more appropriate for this purpose, in which

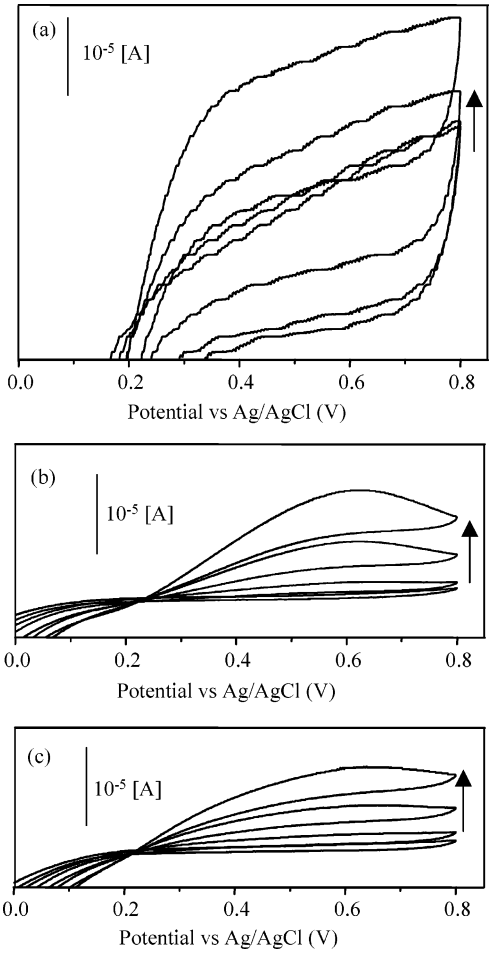

Figure 5. Cyclic voltammograms of hydrogen peroxide on a HMDS PPF-coated Pt electrode: (a) bare, (b) 100 W of deposited power, and (c) 250 W of deposited power. Film thickness: 7 nm. Deposited pressure: 0.6 Pa. The direction of the arrows represents the increment of concentration (0, 0.1, 0.37, and 0.69 mM).

the sputtering of thin films and their surface modifications with the plasma polymerization are carried out sequentially at a batch. It can also be found that when two films deposited by two different conditions (plasma powers) have the same thickness, the one obtained with the lower plasma was larger than the other with the higher. This may be an indication that the lower plasma power results in an internal network structure with a larger sized mesh than the higher power. The other cyclic voltammograms for the other electrochemical species show the same tendency as that in hydrogen peroxide.[30]

Figure 6 shows dose responses of the PPF-coated electrodes to several electrochemical species, dependent upon various plasma powers. Compared with the bare electrodes, the PPF-coated Pt electrodes showed small background currents and slight current increments with increasing additions of the analytes. When J is the observed current and C is the concentration, the slope of each dose response in Figure 6 (J/C, μA/mM) can be defined as the sensitivity (see the Experimental Section), which deceases with the increase of the plasma power.

Figure 7 represents the relative diffusion-controlled selectivity of HMDS PPF coatings toward the tested analytes in terms of the diffusivity ratios of one to another: hydrogen peroxide to catechol ($P_{H_2O_2}/P_{CTL}$), catechol to ascorbic acid (P_{CTL}/P_{AA}), and ascorbic acid to chloropromazine (P_{AA}/P_{CPZ}) formed at various plasma powers. The value of $P_{H_2O_2}/P_{CTL}$ is greater than 3 at a plasma power above 150 W. To the contrary, the ratio value of ascorbic acid to chloropromazine (P_{AA}/P_{CPZ}) arose only at 100 W. For example, PPF deposited at 100 W was compact enough to impede molecules larger than chloropromazine. The size discrimination of the PPF coatings is due to its highly branched network structure and it was possible to control the pore sizes in PPF coatings. In the case of the 7($\pm$0.7)-nm-thick coating, the size exclusion effect was obviously seen with variation of the plasma power, but in the case of the 5($\pm$0.5)-nm-thick coating, it was not the case.[30] As a possible explanation, it is probable that there is a threshold thickness between 5 and 7 nm, where the size exclusion is suddenly achieved. When the thickness of a PPF was greater than 10 nm, the current was too low to be measured. This shows that there is optimal coating thickness around several nanometers which is comparable to the lipid bilayer of the cell membrane. Concerning this, the optimized coating thickness depends on the kinds of membrane thickness. The thickness for acetonitrile and hexadiene PPF was 30$-$50 nm.[18] This indicates that the pore size in HMDS PPF coating is smaller than that in PPF of these monomers; the HMDS PPF (polysiloxane backbone) has a higher cross-linked network than that PPF, which has the matrix of the hydrocarbon backbone.

We also estimated the discrimination effect of the HMDS PPF coatings against the analytes according to their sizes. The cavity size in the HMDS PPF coating was estimated to be 0.57$-$0.71 nm by variable-energy positron lifetime spectroscopy.[31] The maximum cross-sectional area of ascorbic acid was estimated to be 0.67 nm with use of molecular modeling.[32] For hydrogen peroxide, its chemical structure is H$-$O$-$O$-$H, and the bond lengths of O$-$H and O$-$O are 0.096 and 0.146 nm, respectively.[33] Supposing that the molecule has a long chain structure, the maximum size of a hydrogen peroxide molecule would be estimated to be 0.34 nm. The maximum size of catechol and chlorpromazine is ca. 0.52 and 0.92 nm, respectively.[34] From this estimation for the pore sizes in the HMDS PPF, the size discrimination shown between hydrogen peroxide and ascorbic acid appears reasonable. The blocking ability of the PPF coatings is mainly attributed to the size exclusion rather than other effects such as electrostatic and hydrophobic interactions on the scale of these pore sizes ($<$1 nm).[5]

There is no difference in the molecular sizes between ascorbic acid (negatively charged) and dopamine (positively charged).[32] A nitrogen plasma treatment turned the HMDS PPF surface hydrophobic, but did not influence the electrochemical sensitivity.[33] To the contrary, the diffusion model of a relatively slack cross-linking polymer network in which the pore size is larger than 2 nm is dominated by the affinity between the agent and polymer matrix rather than the size discrimination.[5]

To determine the apparent diffusion coefficient (D_{app}) of species through the PPF, chronocoulometry was carried out.[30] In a single experiment, the D_{app} determined by this procedure incorporates (i) diffusion of analyte from the bulk phase to the coating surface, (ii) the partition between the solution and the membrane surface, and (iii) diffusion through the surface of the electrode. The charging and reaction on the surface of the electrode is so fast that it can be ignored. The chronocoulometric charge for oxidizing hydrogen peroxide is shown versus the square root of time in Figure 8. From the Anson's plot, the square of the slope is proportional to the apparent diffusion coefficient (see eq 5). This indicates that the diffusion coefficient of ascorbic acid in the case of the HMDS PPF-coated electrode increased compared with that of the bare electrode.

In the bare electrodes, the diffusion constants of the electrochemical species were estimated as $10^{-5}-10^{-6}$ cm^2/s; the slope

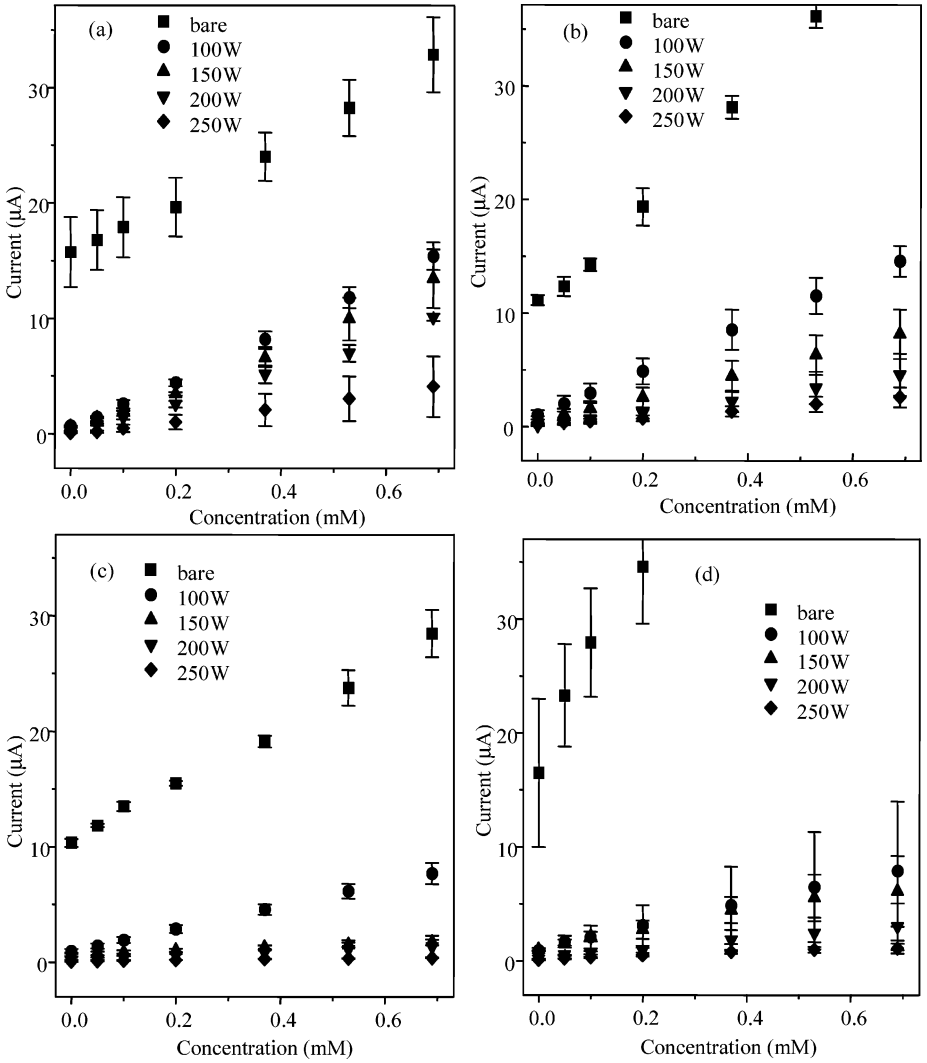

Figure 6. Relation between oxidation current at +700 mV and concentration of various analytes on a HMDS PPF-coated Pt electrode with various deposition powers. Sweep rate: 50 mV s^{-1}. Film thickness: 7 nm. Deposited pressure: 0.6 Pa. Analyte is (a) hydrogen peroxide (H_2O_2), (b) catechol (CTL), (c) ascorbic acid (AA), and (d) chlorpromazine (CPZ). Sensitivities (permeability) *P* are obtained from the slope. (a) $P_{H_2O_2}$(bare, 100W, 150W, 200W, 250W) = 24.6, 21.5, 18.5, 14.0, 5.93 μA mM^{-1}, (b) P_{CTL}(bare, 100W, 150W, 200W, 250W) = 48.5, 19.7, 11.0, 6.41, 3.48 μA mM^{-1}, (c) P_{AA}(bare, 100W, 150W, 200W, 250W) = 25.4, 9.79, 1.51, 1.68 μA mM^{-1}, and (d) P_{CPZ}(bare, 100W, 150W, 200W, 250W) = 91.8, 10.0, 7.58, 4.06, 1.49 μA mM^{-1}.

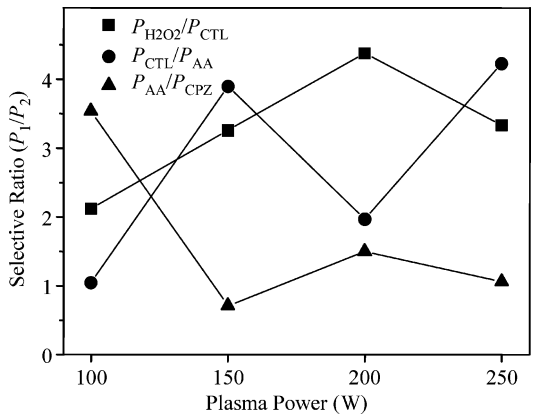

Figure 7. Selective ratio (P_1/P_2) between various analytes on HMDS PPF-coated by electrode with various plasma powers. The *P* is defined as relative permeability to the bare electrode. H_2O_2: hydrogen peroxide. CTL: catechol. AA: ascorbic acid. CPZ: chlororpomazine.

beyond 1 $s^{1/2}$ along the *X*-axis was constant. This value is comparable to that found in the literature.[32] To the contrary, the time profile of the chronocoulometric data for the PPF-coated Pt electrode is distinctively different from that of the bare electrode. The D_{app} values were estimated to be ca. 10^{-8} cm^2/s with the slope in the interval between 0.2 and 0.4 $s^{1/2}$.[30] The diffusion of the analyte through the coating to the electrode surface was not estimated by this method since the membrane was thinner than the diffusion layer (ca. 30.4 nm at a concentration of 0.1 mM).[20] In this case, however, the mass transport of the electrochemical species through the ultrathin PPF is believed to be a rate-determined step. Therefore, we think that the linearity observed during the longer time period represents the diffusion process, although the electrochemical species passes through the nanometer-thick film, which is too thin to be diffusion controlled.

4. Conclusions

The PPF coatings developed in this work were extremely thin, adhered well onto the substrate (electrode), and have a highly cross-linked network structure. Despite the nanothin structure (7 nm), the PPF on an electrode could make a complete coating, which was proved by the AFM images and the XPS data. The mass transport behavior through nanoporous PPF coatings presented a size discrimination effect due to the highly cross-linked network structure. A change of the plasma power gave

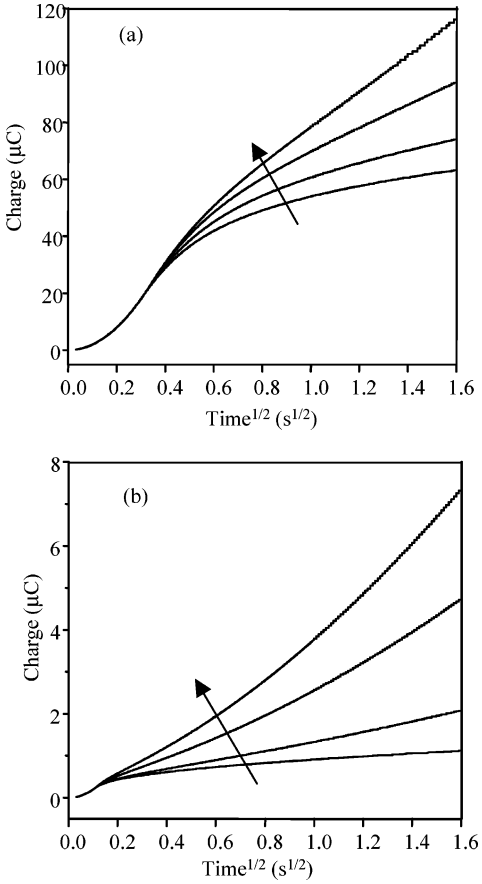

Figure 8. Chronocoulometric plot of ascorbic acid at (a) bare and (b) a HMDS PPF-coated Pt electrode (250 W). Potential step was from 0 to +700 mV. Sampling time was 10 ms. The direction of the arrows represents the increment of concentration (0, 0.1, 0.37, and 0.69 mM).

control over the pore size, capable of suitable programming of the passive mass transport behavior especially in the case of the 7-nm-thick coating. In the case of the 5-nm-thick coating, however, it was not the case. The plasma polymerization occurs in a gas phase of unstable intermediates generated by high energy plasma, and is deposited directly on the substrate as a thin film, whereas the conventional polymers are cast in a solvent. In out experiment, the electrode preparation and the PPF coating were carried out sequentially at a batch, which may be able to offer an opportunity for manufacturing high-quality electrochemical devices. Especially, a sequence of different vacuum processes in a single chamber prevents exposure of the surface of any metal electrode to ambient, which is otherwise prone to surface oxidation. The coating technique is a platform that is flexible in controlling the polymer morphology and the physical properties.

Acknowledgment. This work was partly supported by a research project of Shibaura Institute of Technology. We would like to thank Dr. K.-H. Lee (INNO-SENS, INC., Ann Arbor, MI) for helpful discussions.

Supporting Information Available: Cyclic voltammograms of all kinds of PPF coating electrode toward electron active materials, relation between oxidation current at +700 mV and concentration of various analytes on HMDS PPF-coated Pt electrode (film thickess: 5 nm) with various deposition powers, apparent diffusion coefficient (D_{app}) of the HMDF PPF-deposited Pt electrodes, and visual representation for permeability *P* in PPF-coated Pt electrodes. This material is available free of charge via the Internet at http://pubs.acs.org.

References and Notes

(1) Shard, A. G.; Whittle, J. D.; Beck, A. J.; Brookes, P. N.; Bullett, N. A.; Talib, R. A.; Mistry, A.; Barton, D.; McArthur, S. L. *J. Phys. Chem. B* **2004**, *108*, 12472−12480.
(2) Dhayal, M.; Parry, K. L.; Short, R. D.; Bradley, J. W. *J. Phys. Chem. B* **2004**, *108*, 14000−14004.
(3) Groenewoud, L. M. H.; Engbers, G. H. M.; Feijen, J. *Langmuir* **2003**, *19*, 1368−1374.
(4) Fu, G. D.; Kang, E. T.; Neoh, K. G. *J. Phys. Chem. B* **2003**, *107*, 13902−13910.
(5) Sohn, W.-K.; Ryu, D.-H.; Oh, S.-J.; Koo, J.-K. *J. Membr. Sci.* **2000**, *175*, 163−170.
(6) Inagaki, N.; Kondo, S.; Hirata, M.; Urushihara, H. *J. Appl. Polym. Sci.* **1985**, *30*, 3385−3395.
(7) Ley, V.; Kruzic, A. P.; Timmons, R. B. *J. Membr. Sci.* **2003**, *226*, 213−226.
(8) Yasuda, H.; Lamaze, C. E. *J. Appl. Polym. Sci.* **1973**, *17*, 201−222.
(9) Yasuda, H.; Marsh, H. C.; Brandt, E. S.; Reilley, C. N. *J. Appl. Polym. Sci.* **1976**, *20*, 543−555.
(10) Bell, A. T.; Wydeven, T.; Johnson, C. C. *J. Appl. Polym. Sci.* **1975**, *19*, 1911−1930.
(11) Senda, K.; Vinogradov, G. K.; Gorwadkar, S.; Morita, S. *J. Appl. Phys.* **1993**, *74*, 6425−6426.
(12) Lin, Y.; Yasuda, H. *J. Appl. Polym. Sci.* **1996**, *60*, 543−555.
(13) Yu, Y. J.; Kim, J. G.; Cho, S. H.; Boo, J. H. *Surf. Coat. Technol.* **2003**, *162*, 161−166.
(14) Janča, J.; Sodomka, L. *Surf. Coat. Technol.* **1998**, *98*, 851−854.
(15) Radeva, E. *Sens. Actuators, B* **1997**, *44*, 275−278.
(16) Muguruma, H.; Hiratsuka, A.; Karube, I. *Anal. Chem.* **2000**, *72*, 2671−2675.
(17) Zhang, Z.; Chen, Q.; Knoll, W.; Förch, R. *Surf. Coat. Technol.* **2003**, *174−175*, 588−590.
(18) Hiratsuka, A.; Muguruma, H.; Nagata, R.; Nakamura, R.; Sato, K.; Uchiyama, S.; Karube, I. *J. Membr. Sci.* **2000**, *175*, 25−34.
(19) Stein, W. D. *Transport and Diffusion across Cell Membranes*; Academic Press Inc.: Orlando, FL, 1986.
(20) Bard, A. J.; Faulkner, L. R. *Electrochemical Methods Fundamental and Applications*; John Wiley & Sons: New York, 1980.
(21) Briggs, D.; Seah, M. P. *Practical Surface Analysis by Auger and X-ray Photoelectron Spectroscopy*; John Wiley & Sons: Sussex, UK, 1983; Chapter 9 and Appendix.
(22) Tajima, I.; Yamamoto, M. *J. Polym. Sci., Polym. Chem. Ed.* **1985**, *23*, 615−622.
(23) Krishnamurthy, V.; Kamel, I. L.; Wei, Y. *J. Appl. Polym. Sci.* **1989**, *38*, 605−618.
(24) Sasou, M.; Sugiyama, S.; Yoshino, T.; Ohtani, T. *Langmuir* **2003**, *19*, 9845−9849.
(25) Li, G.; Tobin, J. A.; Denton, D. D. *Appl. Phys. Lett.* **1994**, *64*, 560−562.
(26) Sato, D.; Suwa, T.; Kakimoto, M.; Imai, Y. *J. Photopolym. Sci. Technol.* **1997**, *10*, 149−150.
(27) Tang, J.; Li, J.; Wang, C.; Bai, C. *J. Vac. Sci. Technol. B* **2000**, *18*, 1858−1860.
(28) Roberts, R. F.; Allara, D. L.; Pryde, C. A.; Buchanan, D. N. E.; Hobbins, N. D. *Surf. Int. Anal.* **1980**, *2*, 5−9.
(29) Gooding, J. J.; Praig, V. G.; Hall, E. A. H. *Anal. Chem.* **1998**, *70*, 2396−2402.
(30) The detailed data can be seen in the Supporting Information.
(31) Wang, C. L.; Kobayashi, Y.; Togashi, H.; Kato, K.; Hirotsu, T.; Hirata, K.; Suzuki, R.; Ohdaira, T.; Mikado, T. *J. Appl. Polym. Sci.* **1999**, *74*, 2522−2528.
(32) Tucker, R. C.; Song, I.; Payer, J. H.; Marchant, R. E. *J. Appl. Electrochem.* **1997**, *27*, 1079−1087.
(33) Kase, Y.; Muguruma, H.; Hiratsuka, A.; Karube, I. *IEICE Trans. Electron.* **2004**, *E87-C*, 142−147.
(34) Lee, J.-Y.; Park, S.-M. *J. Phys. Chem. B* **1998**, *102*, 9940−9945.